Design and DSP implementation in HIL of nonlinear observers for a doubly fed induction aero-generator

Bouchaib Rached, Mustapha Elharoussi, Elhassane Abdelmounim, Mounir Bensaid
Laboratory Mathematics, Computer and Engineering Sciences Laboratory (MISI), Faculty of Science and Technology,
Hassan 1st University, Settat, Morocco

Article Info

ABSTRACT

This paper reports on the conception and digital signal processor (DSP)-based hardware-in-the-loop realisation of a nonlinear observer for a grid-connected variable speed wind turbine using a doubly fed induction generator (DFIG). The objective of this work is to build some observation structure based on the extended Kalman filter (EKF), the sliding mode observer (SMO) and the adaptive model reference adaptive system (MRAS) observer to observe certain quantities of the wind power system connected to the electrical grid in order to reduce the complexity and the cost of the hardware, to achieve an increased mechanical robustness, to operate in hostile environments, to have a higher reliability and to ensure an unchanged inertia of the system. The proposed observers will be combined with robust nonlinear controls based on the backstepping approach to control the wind energy conversion system (WECS). The whole will be implemented on a TMS320F28335 DSP board. A comparative analysis of the proposed observers will be carried out. Through the results of the DSP implementation in hardware in the loop (HIL), we will prove that this improved combination increases the desired performance.

Corresponding Author:

Bouchaib Rached
Laboratory Mathematics, Computer and Engineering Sciences Laboratory
Faculty of Science and Technology, Hassan 1st University
Settat, Morocco
Email: bouchaib.rached@gmail.com

NOMENCLATURE

DFIG	: doubly fed induction generator	M	: mutual inductance
EKF	: extended Kalman filter	L_s, L_r	: stator and rotor self-inductance
HIL	: hardware in the loop	ω_r, ω_s	: slip and stator angular velocity
MRAS	: model reference adaptive system	V_{sd}, V_{sq}	: stator voltage
SMO	: sliding mode observer	V_{rd}, V_{rq}	: rotor voltage
WECS	: wind energy conversion system	I_{sd}, I_{sq}	: direct and quadrature stator current
V_{Wind}	: wind speed	I_{rd}, I_{rq}	: direct and quadrature rotor current
R_{wind}	: blade radius	I_{fd}, I_{fq}	: direct and quadrature filter current
Ω_m	: rotational speed	ω_r, ω_s	: slip and stator angular velocity
R_s, R_r	: stator and rotor resistance		

1.   INTRODUCTION

In the midst of climate change, which is mainly related to energy production and consumption, researchers are actively working to develop and design non-polluting and inexhaustible technologies to meet the increased need for electricity. The implementation of such technologies requires the use of renewable energy sources, in particular wind energy. The production of electricity from wind generators is booming and is the fastest growing form of renewable energy. The use of variable speed wind turbines is more widely employed due to their flexibility, efficiency, and energy performance, as well as improved dynamic performance during grid disturbances [1].

Many control technologies have been designed for turbines to optimise their power production for a given wind speed. However, some of these variable speed methods require a wind speed estimation strategy, which is a challenge to perform during high-speed wind variations to be able to derive the maximum power thanks to the maximum power point tracking (MPPT) strategy [2]. For this type of application, the DFIG associated with electronic power converters is today the most used machine [3]. Due to the stochastic nature of the wind, the WECS is equipped with an energy optimisation system. It is in this context that our study intervenes. Thus, we propose to optimise the operation of this system by achieving the following objectives: improve the quality of the electrical power produced; minimise as much as possible the mechanical loads undergone by the drive train; ensure a better energy efficiency; while ensuring the robustness of the control algorithms designed.

The observation of systems allows to estimate the quantities which are not measurable and the observer is the mathematical tool acting as a software sensor, allowing to collect an estimate of the unknown state searched. This estimation can be done in general only with the knowledge of the model of the studied system, but also by the knowledge of the various outputs and inputs of the latter. An intense research activity has been devoted throughout the world to the study of this observation problem and to the resulting synthesis of observers for different types of systems.

The first research on observers was published around the 1960s by Kalman and later by Luenberger [4]–[6]. Since then, researchers have been interested in designing state observers for linear time-invariant systems in a deterministic or stochastic environment. The MRAS method is based on the comparison of quantities obtained in two different ways, on the one hand, by a calculation not explicitly depending on the variable (reference model) and, on the other hand, by a calculation explicitly depending on the variable (adaptive model). This method was developed by Schauder [7]–[10]. Other types of state observers for nonlinear systems were suggested around the 1980s [11]–[14]. First, researchers proposed the synthesis of an observer for a class of nonlinear systems whose error system is linearizable using state transformations that make the nonlinearities of the system dependent only on the inputs and outputs.

In this paper, some optimisations will be made to advanced controls for DFIG using state observers. The proposed observers have been combined with the backstepping approach (Figure 1). This paper is structured as follows. First, the notion of observation will be addressed by discussing the observability of the system under study. Then, the EKF based observer, the SMO and the adaptive MRAS observer will be used to observe some quantities of the wind power system connected to the electrical grid. After that, the implementation of the digital signal processor (DSP) in the loop is presented. In the last section, the results of the validation of the implemented controls are presented.
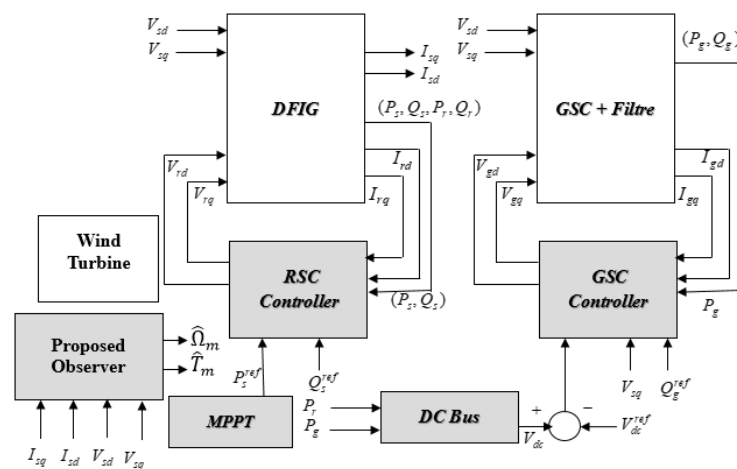

Figure 1. Flowchart of the overall control strategy (observer+controller)

2. METHOD AND MATERIALS

2.1. Modelling of the wind turbine conversion chain based on a DFIG

The most typical connection scheme for the DFIG in a WECS is to supply the stator directly from the grid. While the rotor is powered by two static converters in back-to-back mode (one on the machine side rotor side converter (RSC) and one on the grid side converter (GSC)) as depicted in Figure 2 [15]. The GADA state space model, in the two-phase reference frame, can be written in the following form [16]–[18].

$$\begin{cases} \frac{dI_{sd}}{dt} = \frac{V_{sd}}{\sigma L_s} - \frac{R_s I_{sd}}{\sigma L_s} + \frac{MR_r I_{rd}}{\sigma L_s L_r} - \frac{MV_{rd}}{\sigma L_s L_r} + \omega_s I_{sq} + p\omega \left(\frac{M^2 I_{sq}}{\sigma L_s L_r} + \frac{MI_{rq}}{\sigma L_s} \right) \\ \frac{dI_{sq}}{dt} = \frac{V_{sq}}{\sigma L_s} - \frac{R_s I_{sq}}{\sigma L_s} + \frac{MR_r I_{rq}}{\sigma L_s L_r} - \frac{MV_{rq}}{\sigma L_s L_r} - \omega_s I_{sd} - p\omega \left(\frac{M^2 I_{sd}}{\sigma L_s L_r} + \frac{MI_{rd}}{\sigma L_s} \right) \end{cases} \quad (1)$$

$$\begin{cases} \frac{dI_{rd}}{dt} = \frac{V_{rd}}{\sigma L_r} - \frac{R_r I_{rd}}{\sigma L_r} + \frac{MR_s I_{sd}}{\sigma L_s L_r} - \frac{MV_{sd}}{\sigma L_s L_r} + \omega_r I_{rq} - p\omega \left(\frac{M^2 I_{rq}}{\sigma L_s L_r} + \frac{MI_{sq}}{\sigma L_r} \right) \\ \frac{dI_{sq}}{dt} = \frac{V_{sq}}{\sigma L_r} - \frac{R_r I_{rq}}{\sigma L_r} + \frac{MR_s I_{sq}}{\sigma L_s L_r} - \frac{MV_{sq}}{\sigma L_s L_r} - \omega_r I_{rd} + p\omega \left(\frac{M^2 I_{sd}}{\sigma L_s L_r} + \frac{MI_{rd}}{\sigma L_r} \right) \end{cases} \quad (2)$$

$$\begin{cases} \frac{d\Omega_m}{dt} = \frac{T_m - K \cdot \Omega_m - T_{em}}{J} \\ \frac{dT_{em}}{dt} = \lambda(t) \end{cases} \quad (3)$$

The electromagnetic torque equation is given in (4) [18], [19]:

$$T_{em} = pM \left(I_{rd} I_{sq} - I_{rq} I_{sd} \right) \quad (4)$$

In compact form, (1)-(3) can be rewritten in (5):

$$\begin{cases} \dot{x}(t) = f(x, v, u) + B \cdot \lambda(t) \\ y(t) = h(x) \end{cases} \quad (5)$$

Where:

$B = [0,0,0,0,0,1], x = \left[I_{sd}, I_{sq}, I_{rd}, I_{rq}, \Omega_m, T_{em} \right]^T = [x_1, x_2, x_3, x_4, x_5, x_6]^T$,

$h(x) = [x_1, x_2, x_3, x_4]^T = \left[I_{sd}, I_{sq}, I_{rd}, I_{rq} \right]^T$, $u = \left[V_{rd}, V_{rq} \right]$ $v = [V_{sd}, V_{sq}]$, and $f = [\dot{x}_1, \dot{x}_2, \dot{x}_3, \dot{x}_4, \dot{x}_5, 0]^T$
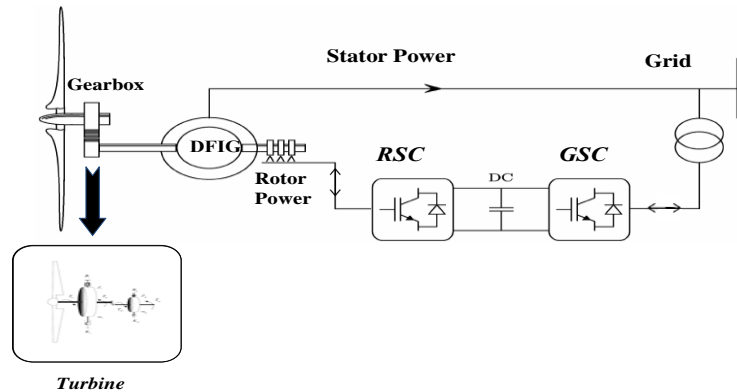

Figure 2. WECS using DFIG

2.2. Study of system observability

The observability of our system requires checking the rank condition which can be written as follows [20]: $\boldsymbol{dim}(\boldsymbol{O})=\boldsymbol{n}=6$. O(x) is the Jacobian of the matrix l(x) defined in (6):

$$O = \frac{\partial l(x)}{\partial x} \quad (6)$$

Where $l(x) = [L_f^0 h \quad L_f^1 h \quad L_f^2 h]^T$, $L_f^0 h = [x_1, x_2, x_3, x_4]^T$, $L_f^1 h = [f_1, f_2, f_3, f_4]^T$, and $L_f^2 h = [grad f_1.f, grad f_2.f, grad f_3.f, grad f_4.f]^T$. The symbol L denotes the Lie derivative of the vector function f(x) in the sense of the vector function h(x). So, the matrix O(x) is a 12×6 matrix represented in (7) [16]:

$$O = \begin{bmatrix} [I_4 \quad 0_{4\times2}] \\ \begin{bmatrix} grad f_1 \\ grad f_2 \\ grad f_3 \\ grad f_4 \end{bmatrix} \\ \begin{bmatrix} grad(grad f_1.f) \\ grad(grad f_2.f) \\ grad(grad f_3.f) \\ grad(grad f_4.f) \end{bmatrix} \end{bmatrix} \tag{7}$$

To ensure the stability of the system, we need to find a 6×6 submatrix of O(x) which will be of full rank, i.e. with a non-zero determinant. Clearly, the first 4 rows are pairwise independent, so they will constitute the first four rows of the submatrix. In addition to these four rows, we take one row of the X sub-matrix and one row of the Y sub-matrix, we find a 6×6 matrix. According to the calculations, sixteen cases are possible to evaluate the observability of the system. Therefore, the Jacobian is of range equal to n if and only if the following conditions are satisfied, as shown in (8):

$$\begin{cases} \varphi_{rd} = I_{rd}L_r + I_{sd}M \neq 0 \\ \varphi_{rq} = I_{rq}L_r + I_{sq}M \neq 0 \end{cases} \tag{8}$$

This leads to the conclusion that the system is observable if and only if the rotor flux is non-zero, i.e. observability is lost at the point where the rotor flux is zero. Therefore, the system is unobservable if:
- The rotor flux tends to zero or, in other words, no electromagnetic torque from the machine.
- The GADA remains at a standstill or does not connect to the electrical grid or, in other words, the rotor and stator currents are almost zero.
- The GADA parameters (M, Lr, Ls) are zero since the machine windings are damaged.

2.3. Observer design
2.3.1. Extended Kalman observer for mechanical torque
The system to be observed is described by the following system as in (9) [21]:

$$\begin{cases} \dot{x}_1 = x_2 - \frac{T_{em}}{J} - \frac{K \cdot x_1}{J} \\ \dot{x}_2 = \lambda'(t) \end{cases} \tag{9}$$

x_1 and x_2 represent the rotor angular speed Ω_m and the mechanical torque T_m, respectively.

$$\begin{cases} x_1 = \Omega_m \\ x_2 = \frac{T_m}{J} \end{cases} \tag{10}$$

In compact form, (9) can be rewritten as in (11):

$$\begin{cases} \dot{X} = A \cdot X + B \cdot T_{em} \\ y = C \cdot X \end{cases} \tag{11}$$

Where $X = (x_1 \quad x_2)^T$, $A = \begin{pmatrix} \frac{-K}{J} & 1 \\ 0 & 0 \end{pmatrix}$, $B = \begin{pmatrix} -1/J \\ 0 \end{pmatrix}$, and $C = (1 \quad 0)$. Consider the following Kalman observer:

$$\begin{cases} \dot{\hat{X}} = A \cdot \hat{X} + B \cdot T_{em} + H \cdot (y - C \cdot \hat{X}) \\ \hat{y} = C \cdot \hat{X} \end{cases} \tag{12}$$

The vector H is composed by: $H = (h_1 \quad h_2)^T$. The estimation error is given by: $\tilde{X} = (\hat{X} - X)$. The dynamics of the error is governed in (13):

$$\dot{\tilde{X}} = \dot{X} - \dot{\hat{X}} = (A - H \cdot C) \cdot \tilde{X} \tag{13}$$

With a judicious choice of the vector H, the matrix $A_0 = A - H.C$ can be introduced. H is chosen as a Hurwitz matrix to ensure exponential convergence in a finite time of the error $\tilde{X} = (\hat{X} - X)$ to 0. The estimated values of states x₁ and x₂ are expressed by (14):

$$\begin{cases} \dot{\hat{x}}_1 = \frac{-K}{J} \cdot \hat{x}_1 + \hat{x}_2 - \frac{1}{J} T_{em} + h_1 \cdot \tilde{x}_1 \\ \qquad \dot{\hat{x}}_2 = h_2 \cdot \tilde{x}_1 \end{cases} \tag{14}$$

The estimated value of the mechanical torque is expressed by: $\hat{T}_m = J.\hat{x}_2$.

2.3.2. Higher order sliding mode observer for mechanical torque

Consider the second order SMO, given by relation (15) based on the super-twisting algorithm [22], where x represents the image of the mechanical torque, be such that: $\hat{T}_m = J.x$.

$$\begin{cases} \dot{\hat{\Omega}}_m = x - \frac{K}{J}\Omega_m - \frac{T_{em}}{J} - A_1|\hat{\Omega}_m - \Omega_m|^{\frac{1}{2}} sign(\hat{\Omega}_m - \Omega_m) \\ \qquad \dot{x} = -A_2 sign(\hat{\Omega}_m - \Omega_m) \end{cases} \tag{15}$$

The two coefficients A₁ and A₂ represent synthesis parameters of the observer. Let the following observation error be:

$$e_{\Omega_m} = (\hat{\Omega}_m - \Omega_m) \tag{16}$$

Let be then:

$$\begin{cases} \ddot{e}_{\Omega_m} = -\frac{\dot{T}_m}{J} + \dot{u} \\ u = x - A_1|e_{\Omega_m}|^{\frac{1}{2}} sign(e_{\Omega_m}) \end{cases} \tag{17}$$

If A₁ and A₂ are chosen with the following conditions as shown in (18):

$$\begin{cases} A_1 > \Phi_1 \\ A_2^2 \geq \frac{4\Phi_1(A_1 + \Phi_1)}{(A_1 - \Phi_1)} \end{cases} \tag{18}$$

Where Φ_1 is a positive constant that satisfies $\left|\frac{\dot{T}_m}{J}\right| < \Phi_1$, this guarantees finite time convergence of e_{Ω_m} to 0. Thus, an approximation of the aerodynamic torque by $\hat{T}_m = J.\hat{x}$ can be derived.

2.3.3. Rotor speed estimation by a new structure of MRAS

The adaptive system to the reference model is based on the matching of two estimators' outputs. The first, which does not present the quantity to be estimated (the speed), is known as the reference model and the second is known as the adjustable model [9], [10], [23]. The error between these two models leads to an adaptation procedure that generates the speed by using the Lyapunov theory or the Popov hyperstability criterion. This speed is used in the adjustable model. From the equations describing the model of the system, the reference model is defined by the (19):

$$\begin{cases} \frac{d\Phi_{rd}}{dt} = \frac{L_r}{M}\left(V_{sd} - R_s I_{sd} - \sigma L_s \frac{dI_{sd}}{dt}\right) \\ \frac{d\Phi_{rq}}{dt} = \frac{L_r}{M}\left(V_{sq} - R_s I_{sq} - \sigma L_s \frac{dI_{sq}}{dt}\right) \end{cases} \tag{19}$$

While the adjustable model is determined by the following system (20):

$$\begin{cases} \frac{d\widehat{\Phi}_{rd}}{dt} = \frac{-1}{T_r}\widehat{\Phi}_{rd} - \widehat{\omega}_r\widehat{\Phi}_{rq} + \frac{L_m}{T_r}I_{sd} \\ \frac{d\widehat{\Phi}_{rq}}{dt} = \frac{-1}{T_r}\widehat{\Phi}_{rq} - \widehat{\omega}_r\widehat{\Phi}_{rd} + \frac{L_m}{T_r}I_{sq} \end{cases} \tag{20}$$

Thus, we have proposed two laws to estimate both the speed and the rotor resistance, Figure 3. $k_{pwr}, k_{pR_s}, k_{iwr}$ et k_{iR_s} are the gains of the two PI controllers forming the adaptation mechanisms.
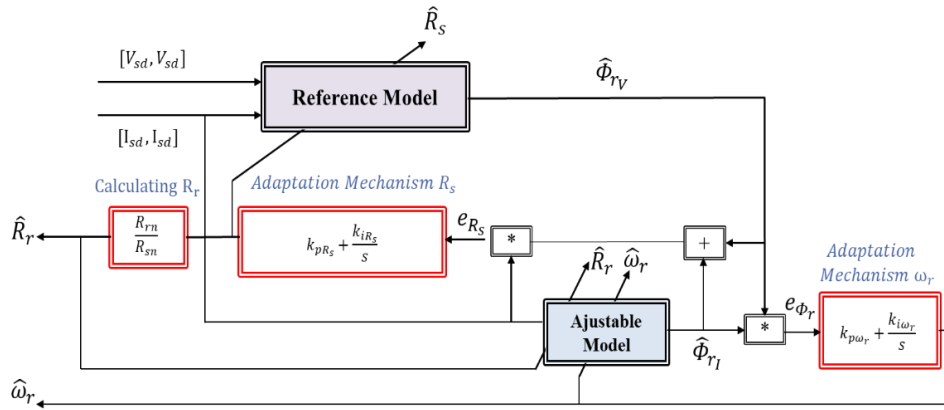
Figure 3. New structure of the MRAS-mutuel observer

2.4. Backstepping control

To present the synthesis of the control laws by backstepping, we start by tracking the maximum power point. The purpose is to design a controller to ensure that the torque follows an optimal torque reference. By defining the error variable as the tracking error. Thus we are provided with a control law allowing the torque to converge towards its reference (Figure 4).
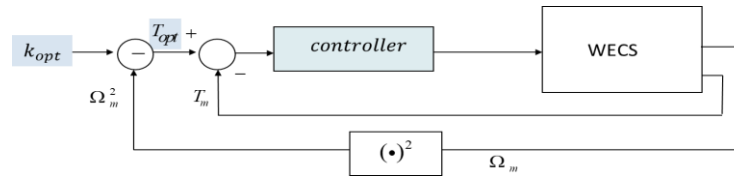
Figure 4. MPPT controller structure

Subsequently we controlled the inverter on the machine side (RSC) in order to follow the power references. Since the control inputs are dependent on the currents, we developed the control in 2 steps. In the first step, we calculated the references of the currents so that the powers follow their references. And in the second step, we calculated the control signals so that the currents follow their references. Thus, we obtained, in the first step (21), the current references, and in the second step (22), the voltage references.

$$\begin{cases} I_{rq}^{ref} = \frac{\sigma L_s L_r}{V_s M R_r}\left[k_1 e_1 + \frac{dP_s^{ref}}{dt} + \frac{\sigma M L_r V_s}{L_s}(V_{rq} - \sigma L_r \omega_r I_{rd} - gV_s\frac{M}{L_s})\right] \\ I_{rd}^{ref} = \frac{\sigma L_s L_r}{V_s M R_r}\left[k_2 e_2 + \frac{dQ_s^{ref}}{dt} + \frac{\sigma L_r L_s}{M V_s}(V_{rd} + \sigma L_r \omega_r I_{rq})\right] \end{cases}, \begin{cases} e_1 = P_s^{ref} - P_s \\ e_2 = Q_s^{ref} - Q_s \end{cases} \tag{21}$$

$$\begin{cases} V_{rq}^{ref} = \sigma L_r\left[k_4 e_4 + \frac{dI_{rq}^{ref}}{dt} + \frac{1}{\sigma L_r}(R_r I_{rq} + \sigma L_r \omega_r I_{rd} + \frac{gM V_s}{L_s})\right] \\ V_{rd}^{ref} = \sigma L_r\left[k_3 e_3 + \frac{dI_{rd}^{ref}}{dt} + \frac{1}{\sigma L_r}(R_r I_{rd} - \sigma L_r \omega_r I_{rq})\right] \end{cases}, \begin{cases} e_3 = I_{rd}^{ref} - I_{rd} \\ e_4 = I_{rq}^{ref} - I_{rq} \end{cases} \tag{22}$$

Where k_1, k_2, k_3 and k_4 are positives constants. For the GSC, we have controlled the inverter in such a way that: the DC bus voltage remains constant and the reactive power in the filter is zero. As the control inputs depend on the currents, we have developed the control in 2 steps (Figure 5). Thus, after the calculation of the two steps, we have developed the following two control signals as shown in (23).

$$\begin{cases} V_{fd}^{ref} = -L\left[k_5 e_5 + \dfrac{dI_{fd}^{ref}}{dt} + \dfrac{R}{L}I_{fd} - \omega_s I_{fq}\right] \\ V_{fq}^{ref} = -L\left[k_6 e_6 + \dfrac{dI_{fq}^{ref}}{dt} + \dfrac{R}{L}I_{fq} + \omega_s I_{fd} - \dfrac{V_{sq}}{L}\right] \end{cases} \tag{23}$$
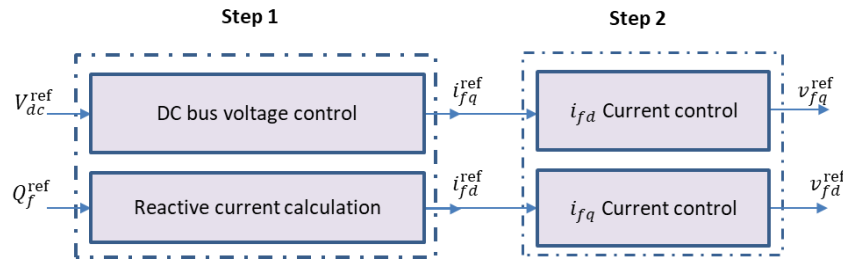
Figure 5. Grid side power converter control diagram

2.5. Implementation of the controller's algorithms on DSP

To validate the designed algorithms, we proposed a co-simulation platform DSP in the Loop using the Matlab simulink environment and the DSP board. Where the system model under simulink interacts with the control laws implemented in DSP (Figure 6). We used the HIL technique. This is a way to test the program running in the DSP without needing a real wind system platform.

To implement the algorithms, we used the eZdspTMSF28335 board (Figure 7). It is a standalone board equipped with a floating point DSP TMS320F28335. It includes a real-time control workshop supported by SIMULINK/MATLAB: TI C2000 DSP [24], [25]. For the programming, we used the code composer studio (CCS). Figure 8 depicts the WECS model under MATLAB/SIMULINK communicating with the DSP and Figure 9 displays the controls HIL interacting with SIMULINK [26], [27].
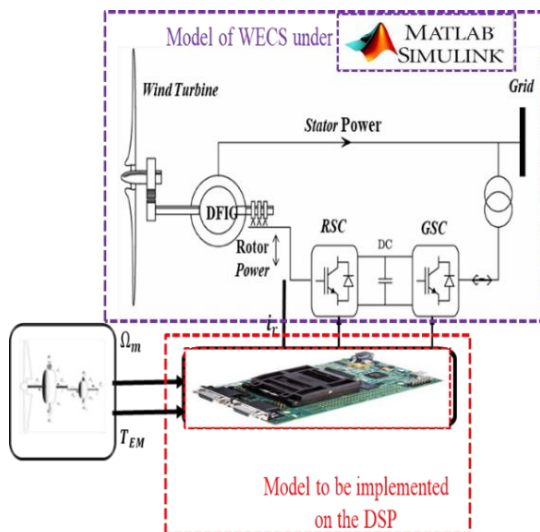

Figure 6. Co-simulation using DSP as a HIL of the control laws and algorithms
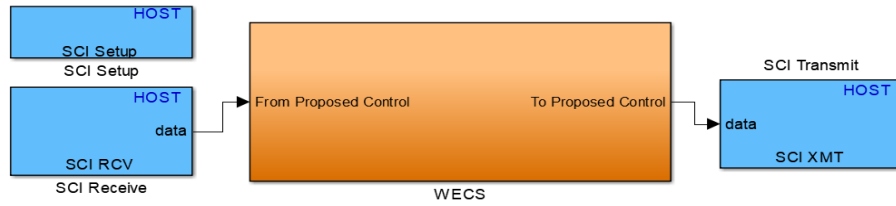

Figure 7. eZDSP TMS320F28335

Figure 8. Model of WECS under MATLAB/SIMULINK

Figure 9. Control algorithms HIL

3. VALIDATION RESULTS

The designed non-linear observers are used in combination with advanced non-linear controls based on the backstepping approach to manage the grid-connected DFIG-based WECS. The combination is implemented in a TMS320F28335 DSP board [24]. To approximate the reality of the stochastic nature of the wind in the experiments, the wind speed is multiplied by the output of a random generator (Figure 10). Figures 11 and 12 show the test results, rotor speed and electromagnetic torque, for the SMO, MRAS observer and EKF observer when the wind speed is varied. This wind speed range covers almost the entire DFIG speed range (i.e. ±25% around the synchronous speed).
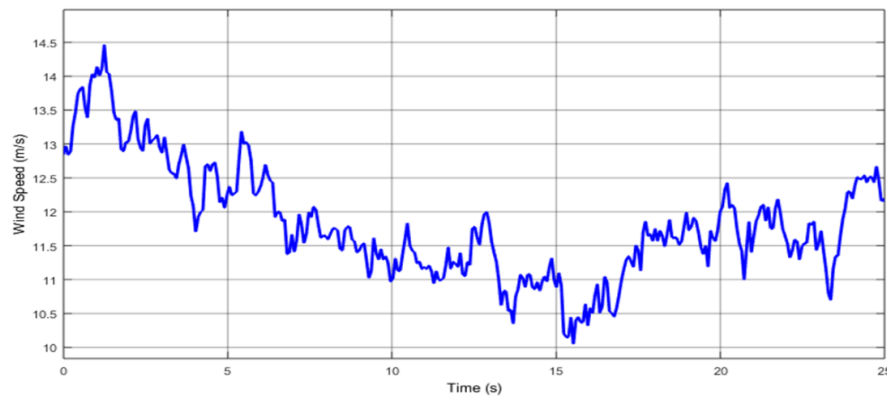
Figure 10. Wind profile used to test the performance of the MRAS, EKF and SMO observers
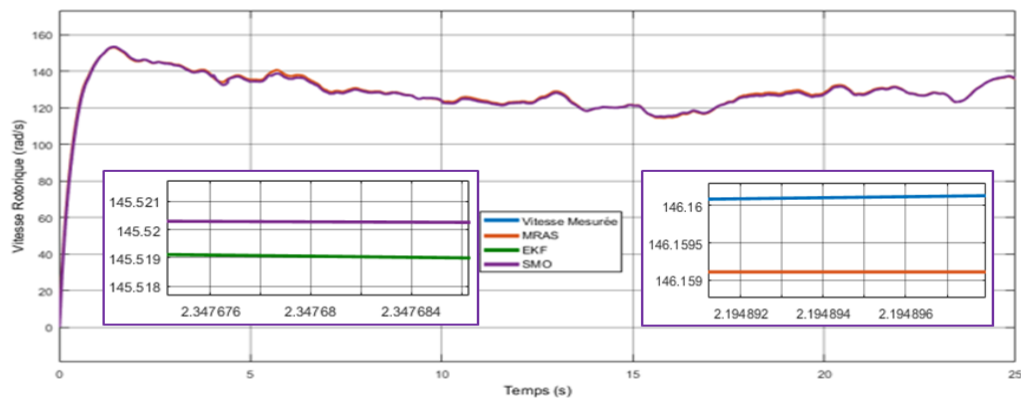
Figure 11. Evolution of the real and estimated rotor speed by the MRAS, EKF, and SMO observers

Design and DSP implementation in HIL of nonlinear observers for a doubly fed … (Bouchaib Rached)
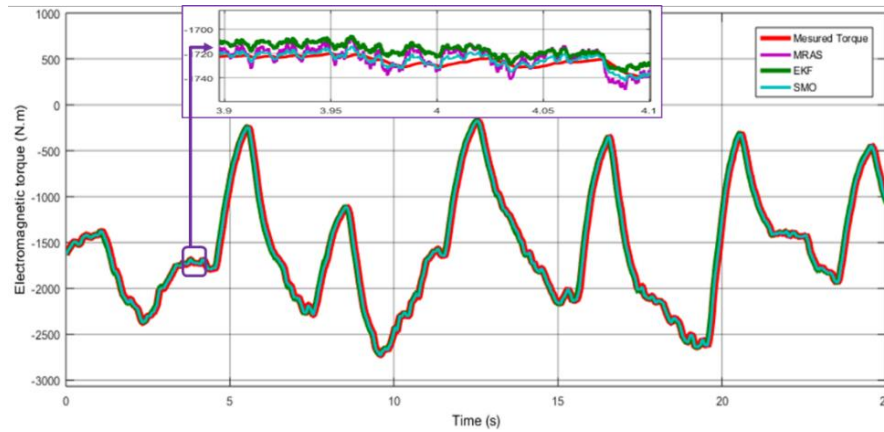
Figure 12. Evolution of the real and estimated electromagnetic torque by the MRAS, EKF and SMO observers

As listed in Table 1, the modified MRAS has a low estimation error compared to the other two observers. Also to be noted, the EKF is slightly sensitive to noise when compared to the other two. According to the Figures 13 and 14, depicting the current evolution, good performance of the proposed combination of MRAS observer and backstepping control through the rotor and stator currents has been observed. These currents vary as a function of speed change without overshoot and with a fast convergence time.

Table 1. Comparative estimation error of the MRAS, EKF and SMO observers

Observer	Estimation error (%)
MRAS	1.7
EKF	2.9
SMO	2.1
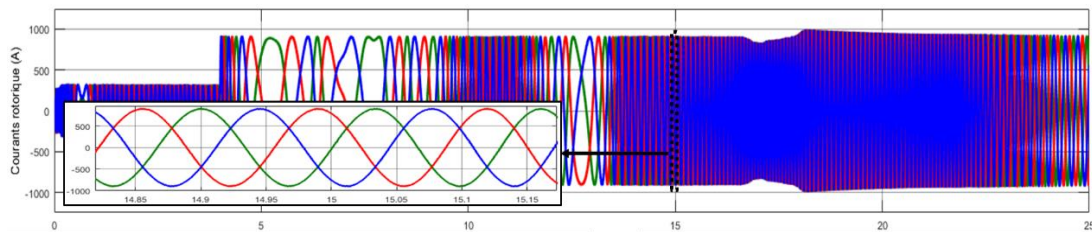
Figure 13. Evolution of the rotor current under a random variation of the wind speed and the reactive power demand
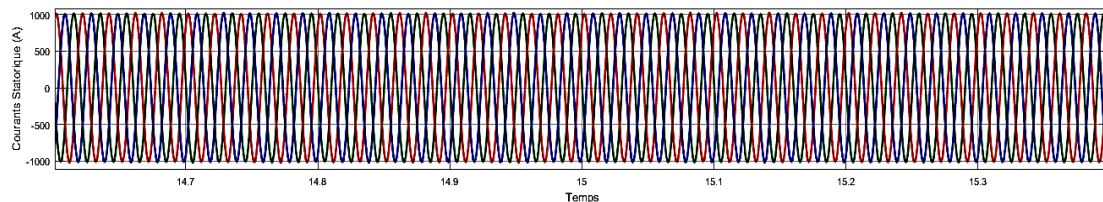
Figure 14. Evolution of the stator current under a random variation of the wind speed and the reactive power demand

The observation error of the variables has no relevant impact on the quality performance of the powers switched between the inverter system and the power grid as indicated in Figure 15. This proves the effectiveness of the decoupling strategy in monitoring the active and reactive powers separately. Thus, the quality of the power produced is verified by a harmonic analysis of the currents in the windings of the machine (Figure 16).
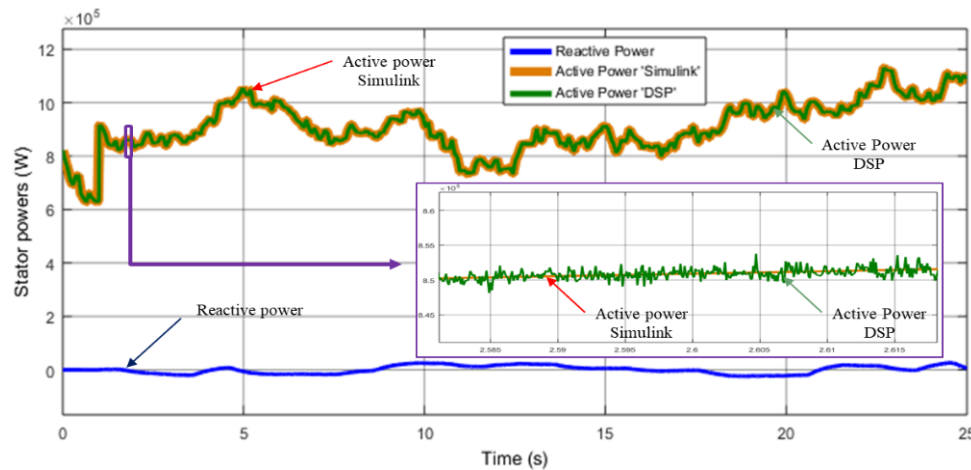
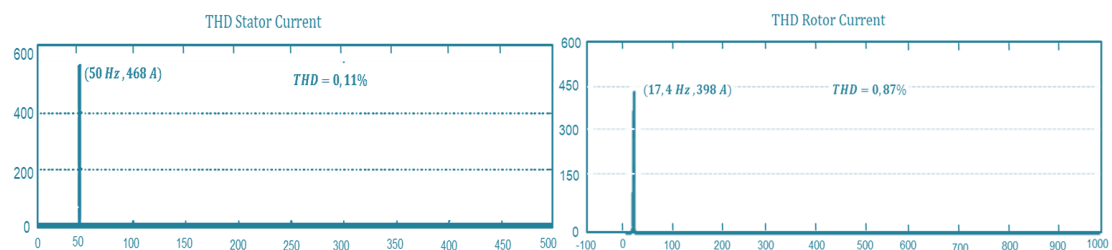Figure 15. Evolution of active and reactive power exchanged between the wind turbine and the grid

Figure 16. Harmonic analysis of the simple currents created in the stator and rotor

4. CONCLUSION

In this work, the observability of the DFIG used in the wind power conversion system was studied using the generic observability rank criterion. Indeed, this study concluded that the DFIG is observable when the rotor fluxes are not zero. This means that the machine grandeurs are observable from the measurements of the stator and rotor currents and voltages if the machine is connected to the electrical grid. This has led to some improvements in the WECS controls by synthesising observers based on the EKF, the SMO and the adaptive MRAS observer.

A simulation and an experimental validation on the DSP in co-simulation (HIL) confirmed the significant improvements brought by the proposed observers. The designed observers have been combined with the backstepping approach. Based on the results of the DSP implementation in HIL, it was shown that this improved association enhances the required performance.

REFERENCES

[1]   O. P. Bharti, R. K. Saket, and S. K. Nagar, "Controller design for DFIG driven by variable speed wind turbine using static output feedback technique," *Engineering, Technology & Applied Science Research*, vol. 6, no. 4, pp. 1056–1061, 2016, doi: 10.48084/etasr.697.
[2]   A. Tamaarat and A. Benakcha, "Performance of PI controller for control of active and reactive power in DFIG operating in a grid-connected variable speed wind energy conversion system," *Frontiers in Energy*, vol. 8, no. 3, pp. 371–378, 2014, doi: 10.1007/s11708-014-0318-6.
[3]   Belkacem, N. Bouhamri, L. A. Koridak, and A. Allali, "Fuzzy optimization strategy of the maximum power point tracking for a variable wind speed system," *International Journal of Electrical and Computer Engineering (IJECE)*, vol. 12, no. 4, pp. 4264–4275, 2022, doi: 10.11591/ijece.v12i4.pp4264-4275.
[4]   R. E. Kalman, "A new approach to linear filtering and prediction problems," *Journal of Basic Engineering*, vol. 82, no. 1, pp. 35–45, 1960, doi: 10.1115/1.3662552.
[5]   R. E. Kalman and R. S. Bucy, "New results in linear filtering and prediction theory," *Journal of Basic Engineering*, vol. 83, no. 1, pp. 95–108, 1961, doi: 10.1115/1.3658902.
[6]   D. Luenberger, "An introduction to observers," *IEEE Transactions on Automatic Control*, vol. 16, no. 6, pp. 596–602, 1971, doi: 10.1109/TAC.1971.1099826.
[7]   S. Abdeddaim, A. Betka, S. Drid, and M. Becherif, "Implementation of MRAC controller of a DFIG based variable speed grid connected wind turbine," *Energy Conversion and Management*, vol. 79, pp. 281–288, 2014, doi: 10.1016/j.enconman.2013.12.003.

[8]   B. Targui, O. H. -González, C. M. A. -Zaragoza, M. E. G. -Sánchez, and G. V. -Palomo, "Observer for a class of Lipschitz nonlinear systems with multiple time-varying delays in the nonlinear measured outputs," *Asian Journal of Control*, vol. 24, no. 3, pp. 1122–1132, 2022, doi: 10.1002/asjc.2537.

[9]   M. S. Zaky, M. K. Metwaly, H. Z. Azazi, and S. A. Deraz, "Performance of a modified stator current based model reference adaptive system observer in sensorless induction motor drives," *Electric Power Components and Systems*, vol. 46, no. 16–17, pp. 1857–1871, 2018, doi: 10.1080/15325008.2018.1527866.

[10]   G. Brando, A. Dannier, and I. Spina, "A full order sensorless control adaptive observer for doubly-fed induction generator," in *2019 International Conference on Clean Electrical Power (ICCEP)*, 2019, pp. 464–469, doi: 10.1109/ICCEP.2019.8890195.

[11]   J. P. Gauthier and I. A. K. Kupka, "Observability and observers for nonlinear systems," *SIAM Journal on Control and Optimization*, vol. 32, no. 4, pp. 975–994, 1994, doi: 10.1137/S0363012991221791.

[12]   R. Hermann and A. Krener, "Nonlinear controllability and observability," *IEEE Transactions on Automatic Control*, vol. 22, no. 5, pp. 728–740, 1977, doi: 10.1109/TAC.1977.1101601.

[13]   K. Boureguig, A. Mansouri, and A. Chouya, "Performance enhancements of DFIG wind turbine using fuzzy-feedback linearization controller augmented by high-gain observer," *International Journal of Power Electronics and Drive Systems (IJPEDS)*, vol. 11, no. 1, pp. 10–23, 2020, doi: 10.11591/ijpeds.v11.i1.pp10-23.

[14]   C. Edwards, S. K. Spurgeon, and C. P. Tan, "On the development and application of sliding mode observers," in *Variable Structure Systems: Towards the 21st Century*, Berlin, Heidelberg: Springer Berlin Heidelberg, 2002, pp. 253–282, doi: 10.1007/3-540-45666-X_11.

[15]   B. Rached, M. Elharoussi, and E. Abdelmounim, "Design and investigations of MPPT strategies for a wind energy conversion system based on doubly fed induction generator," *International Journal of Electrical and Computer Engineering (IJECE)*, vol. 10, no. 5, pp. 4770–4781, 2020, doi: 10.11591/ijece.v10i5.pp4770-4781.

[16]   A. A. R. Al Tahir, R. Lajouad, F. Z. Chaoui, R. Tami, T. Ahmed-Ali, and F. Giri, "A Novel Observer Design for Sensorless Sampled Output Measurement: Application of Variable Speed Doubly Fed Induction Generator," *IFAC-PapersOnLine*, vol. 49, no. 13, pp. 235-240, 2016, doi: 10.1016/j.ifacol.2016.07.957.

[17]   B. Rached, M. Elharoussi, and E. Abdelmounim, "Fuzzy logic control for wind energy conversion system based on DFIG," in *2019 International Conference on Wireless Technologies, Embedded and Intelligent Systems (WITS)*, 2019, pp. 1–6, doi: 10.1109/WITS.2019.8723722.

[18]   E. N. Sanchez and R. R. -Cruz, *Doubly fed induction generators: control for wind energy*. CRC Press, 2016, doi: 10.1201/9781315368771.

[19]   A. J. Laafou, A. A. Madi, Y. Moumani, and A. Addaim, "Proposed robust ADRC control of a DFIG used in wind power production," *Bulletin of Electrical Engineering and Informatics (BEEI)*, vol. 11, no. 3, pp. 1210-1221, 2022, doi: 10.11591/eei.v11i3.3539.

[20]   L. A. M. -Martínez, C. H. Moog, and M. V. -Villa, "Observability and observers for nonlinear systems with time delays 1," *IFAC Proceedings Volumes*, vol. 33, no. 23, pp. 109–114, 2000, doi: 10.1016/S1474-6670(17)36925-2.

[21]   B. Rached, M. Elharoussi, and E. Abdelmounim, "DSP in the loop implementation of sliding mode and super twisting sliding mode controllers combined with an extended Kalman observer for wind energy system involving a DFIG," *International Journal on Energy Conversion (IRECON)*, vol. 8, no. 1, pp. 26–37, 2020, doi: 10.15866/irecon.v8i1.18432.

[22]   H.-T. Yau, P.-Y. Chen, and Y.-L. Chen, "High order sliding mode control for discrete-time systems with external disturbances," *International Journal of Nonlinear Sciences and Numerical Simulation*, vol. 11, pp. 131–135, 2010, doi: 10.1515/IJNSNS.2010.11.S1.131.

[23]   H. Mabrouk and A. Boumediene, "An efficient predictive current controller with adaptive parameter estimation in 3-ϕ inverter," *International Journal of Power Electronics and Drive Systems (IJPEDS)*, vol. 12, no. 2, pp. 858–869, 2021, doi: 10.11591/ijpeds.v12.i2.pp858-869.

[24]   B. Rached, M. Elharoussi, and E. Abdelmounim, "Implementation of TMS320f28335 DSP code based on SVPWM technique for driving VSI with induction motor," *International Journal on Energy Conversion (IRECON)*, vol. 7, no. 4, p. 136, 2019, doi: 10.15866/irecon.v7i4.17790.

[25]   Enas D. Hassan, Khalid G. Mohammed, Inaam I. Ali, "DSP implementation in the loop of the vector control drive of a permanent magnet synchronous machine," International Journal of Power Electronics and Drive Systems (IJPEDS), vol. 13, no. 3, pp. 1895-1903, 2022, doi: 10.11591/ijpeds.v13.i3.pp1895-1903.

[26]   B. Rached, M. Bensaid, M. Elharoussi, and E. Abdelmounim, "DSP in the loop implementation of the control of a DFIG used in wind power system," in *2020 1st International Conference on Innovative Research in Applied Science, Engineering and Technology (IRASET)*, 2020, pp. 1–6, doi: 10.1109/IRASET48871.2020.9092165.

[27]   H. Afghoul, F. Krim, A. Beddar, and A. Ounas, "Real time implementation of sliding mode supervised fractional controller for wind energy conversion system," in *Renewable Energy for Smart and Sustainable Cities*, Cham: Springer, 2019, pp. 181–191, doi: 10.1007/978-3-030-04789-4_20.

BIOGRAPHIES OF AUTHORS

Bouchaib Rached received his Ph.D degree in Electrical Engineering "automatic, electrotechnics and electronics" in 2022 from Faculty of Science and Technical, Hassan 1st University, Settat, Morocco. In 2016, he successfully passed the external aggregation contest in electrical engineering. He received an engineer's degree in Department of Electrical Engineering from Mohammadia School of Engineering Morocco in 2012. His research activities include the design and implementation in digital calculators of advanced control algorithms of wind energy systems connected to the grid, control strategies for AC machine drives and power quality. He also has research interests ranging from signal processing to industrial applications of automatic control. He can be contacted at email: bouchaib.rached@gmail.com.

Mustapha Elharoussi was born in Azilal Morocco in 1974; he received his Ph.D in error correcting codes from Mohammed V University Morocco in 2013. In 2014 he joined as Professor in Department of Applied Physics at Faculty of Science and Technical, Hassan 1st University, Settat, Morocco. He can be contacted at email: m.elharoussi@gmail.com.

Elhassane Abdelmounim received his Ph.D in applied spectral analysis from Limoges University at Faculty of Science and Technical, France in 1994. In 1996, he joined as Professor, Department of Applied Physics at Faculty of Science and Technical, Hassan 1st University, Settat, Morocco. His current research interests include digital signal processing and machine learning. He is currently coordinator of a Bachelor of Science in electrical engineering and researcher in System Analysis and Information Technology (ASTI) at Faculty of Science and Technical, Hassan 1st University, Settat, Morocco. He can be contacted at email: hassan.abdelmounim@hotmail.fr.
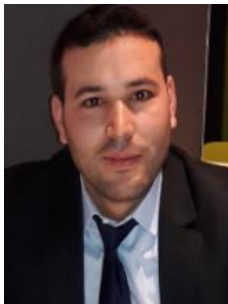
Mounir Bensaid was born in Ouazzane, Morocco. He is a Ph.D student in the Laboratory Mathematics, Computer and Engineering Sciences (MISI) Laboratory, Team: Systems Analysis and Information Processing (ASTI), Faculty of Science and Technical, Hassan 1st University, Morocco. He received the Master in automatic, signal processing and industrial computing from Faculty of Science and Technical, Hassan 1st University, Settat, Morocco in 2018. His research consists in modeling, characterization, control and optimization of multi-drive systems. He can be contacted at email: mo.bensaid@uhp.ac.ma.